



Cost analysis of different vehicle technologies for semi-flexible transit operations

Sushreeta Mishra ^a, Babak Mehran ^{a,*}

^a Department of Civil Engineering, University of Manitoba, 66 Chancellors Cir, Winnipeg, MB R3T 2N2, Canada

ARTICLE INFO

Keywords:

Semi-flexible transit
Battery Electric
Low demand areas
Optimization
Headway
Slack time

ABSTRACT

In low-demand areas, semi-flexible transit system (SFT) operated by battery electric vehicles (BEVs) can reduce operational costs and achieve zero emissions, allowing SFT to be used more widely, and transit agencies to benefit more significantly. This paper is aimed at analyzing the effect of the additional requirements of BEVs on the cost efficiency of SFT services while considering different headways and slack time to accommodate route-deviation. Analytical models are used for detailed estimation of the total cost, including operator, user, and environmental costs, allowing a comparison with internal combustion engine (ICEV) vehicle technology, and three vehicle sizes: minivans, standard vans, and minibuses. Study results can be used to evaluate budget requirements to upgrade an existing ICEV based standard bus service along an underperforming low demand route to a BEV based SFT service. The application of the proposed methodology is demonstrated for a low-demand bus route in Regina, Canada.

1. Introduction

Urban transit systems are quickly adopting electrification because it offers several advantages, such as lower operational expenses, lower energy usage and pollution, and simpler implementation and upkeep (Islam and Lownes, 2019). Several demonstration projects for electric bus operation are currently being conducted in Canada (Mohamed et al., 2018). For instance, three 5.3 m compact electric buses manufactured by Tecnibus, have been operating in Quebec since 2005. A 12.2 m lithium-ion-powered bus developed by Mitsubishi Heavy Industries and the New Flyer is operating on Winnipeg Transit route 20 Academy-Watt. Despite the potential benefits, it is essential to carefully assess the cost-effectiveness of electrification by considering the additional resources required for electric operations as high capital costs and infrastructure costs (charging stations) are the two key factors that hinder the implementation of electric bus technology in the Canadian transit context (Mohamed et al., 2018). As a flexible mobility service, semi-flexible transit (SFT) operates with a fixed/flexible route, stop, and schedule to accommodate a few curb-to-curb stop requests. In response to the growing demand for paratransit services as well as the high operating costs associated with regular bus transit, SFT with route deviations is the most discussed transit alternative for low demand conditions (Koffman, 2004; Weiner, 2008). It is suggested by Diana et al. (2007) that demand responsive transit services minimize emissions in scenarios involving high-quality service levels and low demand density compared to fixed-route services. SFT can maximize the benefits of electrification as it retains the properties of both demand-responsive transit and fixed-route transit in its operation and service design, providing it with the flexibility and adaptability to implement external techniques to minimize operating costs and reduce greenhouse gas emissions. For instance, the high operating

* Corresponding author at: Department of Civil Engineering, University of Manitoba, 66 Chancellors Cir, Winnipeg, MB R3T 2N2, Canada.
E-mail addresses: mishras1@umanitoba.ca (S. Mishra), babak.mehran@umanitoba.ca (B. Mehran).



cost associated with electrification can be offset by shifting paratransit trips to cheaper modes like SFT (Fu, 2002), implementing innovative service delivery models like integrated contracting and in-house service (Mishra et al., 2020), demand optimization (Mehran et al., 2020; S Mishra and Mehran, 2023), and zoning (Kim et al., 2019). Battery electric vehicles (BEVs), powered by electricity stored exclusively in a battery package, can achieve zero emissions, but their design entails additional components, primarily battery capacity and charging strategy, which makes them a more complex powertrain typology than diesel-powered internal combustion engines (ICEV) (Li, 2016). BEVs are typically charged in four ways: overnight charging, fast/opportunity charging, battery swapping, and wireless charging. The cost of battery swapping and wireless charging infrastructures, however, is significantly higher than the cost of the fast-charging system, and overnight charging will require a greater fleet size of small-capacity electric vehicles characteristic of SFT since the maximum allowed battery capacity and vehicle size are limited. Therefore, the BEVs must be off duty until they are fully charged at the overnight charging stations equipped at the depot (Ke et al., 2016). Thus, the opportunity charging strategy is more prevailing and allows BEVs to be recharged without significantly reducing the useful operation time or availability of the vehicle. Additionally, studies implementing opportunity charging focus on two strategies: (a) charging within a single trip assuming consecutive trips are independent and irrelative (Badia and Jenelius, 2021), and (b) charging between multiple trips because the state-of-charge (SoC) of the electric bus after the last trip influences the route range for the following trip (Bektaş et al., 2016).

SFT services are not widely implemented due to their high operating costs, which are primarily caused by smaller vehicle sizes and circuitous routes. In low-demand routes, SFT services are more cost-effective than fixed-route transit services, but in higher-demand routes, the costs outweigh the benefits. However, the adoption of electric vehicles for SFT services could lead to significant reductions in the costs related to energy consumption and the environment, making SFT more competitive and opening new opportunities for wider implementation. Despite the potential benefits, it is essential to carefully assess the cost-effectiveness of electrification by considering the additional resources required for electric SFT operations. This information is crucial for transit agencies to determine the most cost-competitive electric charging technology and to make informed decisions about allocating budgets to upgrade existing standard bus fleets with electric SFT vehicles on low-demand, underperforming bus routes. Furthermore, it's important to note that if transit agencies can create a balance of both cost-effectiveness and environmental benefits, it will be a win-win situation for both the agency and the citizens.

This study aims to determine if utilizing small battery-powered vehicles along with opportunity charging methods for SFT operation can be a viable option in low-demand bus routes. The study investigates the cost-efficiency of different scenarios for SFT operation, broken down by vehicle technology (ICEVs and BEVs) and vehicle size (minivans, standard vans, and minibuses). Analytical models developed to estimate the total system cost, including operator, user, and environmental costs, are used to determine the most efficient flexible design among the above scenarios. Although several design parameters influence SFT, this study focuses on identifying optimal values for two important design parameters: service headway and slack time per trip allocated to accommodate route deviations. Finally, we compare the cost-effectiveness of scenarios to other tailored services based on varying charging speed, demand, battery capacity, and minimum SoC. The application of the proposed analysis method is demonstrated for a low-demand bus route in Regina, Canada.

2. Literature review

Estrada et al. (2021) proposed the first analytical model for determining the optimal vehicle technology for SFT and taxi in the domain of intermediate demand. This model identifies an optimal headway range for semi-flexible transit that minimizes the total cost to the operator and user. Despite capturing some general trends, the models developed failed to capture the details of system behavior as the models do not include essential components like environmental cost, capital costs associated with charging infrastructure, and estimation of additional fleet size requirements due to charging time. Badia and Jenelius (2021) studied the impact of automation and electrification on feeder transit systems serviced by fixed routes and door-to-door services in suburban areas. Analytical models based on continuous approximations are used to identify the configuration of decision variables that minimize total costs per passenger. Due to electrification, the authors modified the cost structure by considering charging time in estimating the fleet size and the number of charging stations. Although extensive, this study estimates fleet size by adding a fixed amount of charging time per cycle, with the conservative assumption that this time cannot overlap with layover time, and it does not consider the impact of battery size variation on operating costs. Barraza and Estrada (2021) developed robust analytical models to design an efficient transit network operated by battery electric and diesel buses in cities with a grid-shaped road network, based on continuous approximations. The study identifies the optimal vehicle size, vehicle technology, and charging strategy that minimizes operator cost, emissions cost, and the travel time of transit users, while optimizing the network design (spatial and temporal coverage) parameters. Estrada et al. (2022) derived analytical operating cost models to estimate the number of resources to be deployed for different vehicle powertrain technologies and charging schemes. Costs incurred by the transit agency include vehicle depreciation and labor, battery cost, distance cost, and charging infrastructure cost. Several charging schemes are evaluated for battery electric vehicles, including (a) day charging at bus garages with and without advancing the charging period to reduce fleet sizes during peak hours, and (b) opportunity charging at electric stations located at both or one end or terminal stop with or without skipping charging operations during peak hours. Although the above-cited studies evaluated the cost-effectiveness of vehicle technology and charging scheme using an analytical model that modified the cost structure due to electrification, many studies concerning demand-responsive transit focus on autonomous electric vehicles (Militão and Tirachini, 2021) and estimate the change in unit cost parameters with the level of automation or use aggregated annual costs or simulation for estimation (Bösch et al., 2018; Schlüter et al., 2021).

Table 1 provides a summary of the existing research reviewed that is essential to highlight the gaps in the literature. Previous research has shown that SFT is cost-effective under low-demand conditions and regular bus transit is cost-effective under high-demand

conditions (Mehran et al., 2020; Mishra et al., 2020). However, studies that focus on optimizing tactical or strategic planning variables such as headway and slack time for SFT are limited, despite Alshalalfah (2009) and Fu (2002) suggesting that they have some interaction. Mishra and Mehran (2023) jointly optimized slack time and headway for an ICEV-based SFT system serving regular transit and paratransit passengers simultaneously. These studies also do not consider the use of electric vehicles or automation technology. This study aims to fill this gap by investigating whether electrifying SFT is economically feasible, and specifically focusing on the optimization of slack time and headway for a battery-electric vehicle-based SFT.

Although the purpose of this study is to compare alternative powertrain technologies for SFT using analytical cost models, the state-of-the-art solution algorithms implemented at various levels of decision-making (operational, tactical, and strategic) for electric vehicle-based demand responsive transit include mixed integer linear programming, constrained optimization, metaheuristics, stochastic/robust optimization, and reinforcement learning and is discussed in detail in Ma and Fang (2022).

3. Service description

The defined transit system is based on the following assumptions:

A: *Service area*- The service area is modeled as a rectangle with dimensions W (km) and L (km) (see Fig. 1(a)). The rectangular service area is an approximation of similar shapes to get a closed-form solution, and this approximation is used in similar works (Daganzo, 2005; Estrada et al., 2021; Fu, 2002). While the rectangular area should realistically represent many practical situations of low demand route comprising of majorly residential area, further research might be needed for other shape types.

B: *Operating policy*- We adopt the route-deviation policy defined by Koffman (2004) where vehicles follow a fixed route and deviate to serve curb-to-curb requests, with a maximum allowable deviation of $W/2$ on both sides (see Fig. 1).

C: *Demand distribution*- The passenger demand is assumed to be uniformly and independently distributed along the route and the boarding and alighting pattern at a stop is assumed to be Poisson distributed.

These assumptions are examined in the studies discussed in detail below, and the results indicate that these assumptions are valid for this study focusing on a low demand route. Mishra et al. (2020) investigated the effect of non-uniformity in demand distribution along a low demand route using Poisson binomial distribution to ensure that the probability of stopping at each stop is independent and non-identical. Study results suggest that, for low demand, less than 20 pass/hr, there is no noticeable gap in the expected number of vehicle stoppings (i.e., $E(s)$) observed for SFT; therefore, in-vehicle time remains the same. However, the study assumed Poisson passenger arrival pattern at stops and suggested that for low demand route adopting the lower limit of $E(s)$ (refer Appendix A) estimated at twice the number of passengers boarded in the vehicle is a slight underestimate of the operator's cost (i.e., error is -10% for 1 pass/hr, approaches rapidly to 0% at 20 pass/hr, and then gradually increases for demand > 20 pass/hr). Mishra et al. (2023) examined whether a negative-binomial distribution with overdispersion would be more indicative of a route with low demand and a Poisson distribution would be characteristic of a route with high demand. For demand less than 20 pass/hr, both distributions predict the same $E(s)$; however, for medium range demand, the gap widens and Poisson distribution overestimates $E(s)$, while both distributions converge for higher demand ranges.

D: *Request type*- Within the service area, passenger pick-up/drop-off requests are of two types: flag stops, and curb-to-curb stops and passengers can request service in four possible types with proportions of γ_1 , γ_2 , γ_3 , and γ_4 ($\gamma_1 + \gamma_2 + \gamma_3 + \gamma_4 = 1$) as follows:

Table 1
Summary of reviewed studies.

Reference	System	Method	Objective	Decision variable	Technologies	Vehicle size
Estrada et al. (2021)	FBT, SFT, DRT	AN	Minimize OC and UC	headway, waiting time, and stop spacing	EV, ICEV, AV	standard bus ($C = 70$), minibus ($C = 20$), taxi ($C = 4$)
Badia and Jenelius (2021)	FBT, DRT	AN	Minimize OC and UC	headway, line spacing, stop spacing, vehicle size	EV, AV	6 sizes: micro bus ($C = 12$) to articulated bus ($C = 120$)
Barraza and Estrada (2021)	FBT	AN	Minimize OC, UC, and EC	headway, line spacing, stop spacing, number of chargers	EV, ICEV	standard bus ($C = 70$), articulated bus ($C = 120$)
Estrada et al. (2022)	FBT	AN	Minimize OC	fleet size and number of charging stations	EV, ICEV, HEV	standard bus ($C = 70$), articulated bus ($C = 120$)
Militão and Tirachini (2021)	DRT	AN & NM	Minimize OC and UC	fleet size, vehicle capacity	EV, AV	car ($C = 5$), van ($C = 8$), minibus ($C = 44$)
Bösch et al. (2018)	DRT	AN	Minimize OC	vehicle technology	EV, AV	solo ($C = 1$), midsize ($C = 4$), van ($C = 8$), minibus ($C = 20$)
Schlüter et al. (2021)	DRT	AN	Minimize OC, UC, and EC	fleet size	AV	minivan ($C = 6$)
Alshalalfah (2009)	SFT	AN & SM	Minimize OC, UC, and Maximise SB	service area and slack time	ICEV	van ($C = 8$)
Fu (2002)	SFT	AN & SM	Minimize OC, UC, and Maximise SB	slack time	ICEV	minibus ($C = 20$)
This study	SFT	AN	Minimize OC and UC	headway and slack time	EV, ICEV	mini-van ($C = 7$), standard van ($C = 15$), mini-bus ($C = 25$)

System: FBT- Fixed route bus transit, DRT- demand responsive transit (door-to-door service), SFT- semi-flexible transit; *Method:* NM- Numerical, HT- Heuristic, SM- Simulated, AN- Analytical; *Objective:* OC- Operating cost, UC- User cost, EC- Environmental cost, SB- Service benefit; *Technologies:* EV- Electric vehicle, ICEV- diesel-powered internal combustion engines, HEV- Hybrid electric vehicle, AV- Autonomous vehicle

Type 1: Both pick-up and drop-off locations are along the fixed route (Both flag stops).

Type 2: Pick-up location deviates from the fixed route and the drop-off location is along the fixed route (flag stop and curb-to-curb stop).

Type 3: Drop-off location deviates from the fixed route and the pick-up location is along the fixed route (flag stop and curb-to-curb stop).

Type 4: Both pick-up and drop-off locations deviate from the fixed route (Both curb-to-curb stops).

E: *Vehicle capacity*- We consider three common vehicle types in SFT with varying capacities: (a) Mini-van (7-passenger vehicle excluding the driver), (b) standard van (15-passenger vehicle excluding the driver), and (c) mini-bus (25-passenger vehicle excluding the driver).

F: *Charging scenarios*- In this study, the opportunity charging scheme is considered with the following strategy: vehicles are charged after the state-of-the-charge (SoC) of the battery drops to a minimum value. In this case, fast charging stations may be deployed at the last stop/terminal or located at L_D units of distance away from the terminal station (see Figure 1). Thus, for recharging if $L_D > 0$, each vehicle travels an L_D kilometer from and to the terminal station before serving the next trip.

G: *Vehicle technology*- We focus on comparing the costs of systems composed of (a) internal combustion engine vehicles (ICEV) and (b) battery electric vehicles (BEV). ICEVs are powered by a conventional internal combustion engine, typically using fossil fuels such as gasoline or diesel. BEVs are powered by chemical energy that is stored in an onboard lithium-ion-based battery package, which is charged by connecting a plug to an external power source.

4. Cost calculation

4.1. Operator cost

C_{OC} in Eq. (1) is calculated as the sum of (a) time-related vehicle costs including amortized vehicle cost, labor, and staff costs, vehicle depreciation, and insurance (b) distance-related costs including energy and maintenance costs, (c) time-related battery cost mainly purchase cost and the depreciation cost of batteries (i.e., typically, time-related vehicle costs does not encompass the depreciation cost of batteries since the battery life is significantly lower than the vehicles), and (d) time-related charging or refueling infrastructure cost mainly installation cost and depreciation cost.

$$C_{OC} = C_1 \times F + C_2 \times L_F + C_3 \times E_b \times F + C_4 \times N_{st} \quad (1)$$

Here, C_1 is unit temporal cost (\$/veh-hr), C_2 is unit distance cost (\$/veh-km), C_3 is unit temporal battery cost (\$/kWh-hr), C_4 is unit charging facility cost or refueling station cost (\$/charger-hr), F is fleet size, L_F is vehicle kilometers traveled by fleet per unit time (veh-km/hr), E_b is battery capacity per vehicle (kWh /veh), and N_{st} is the number of charging or refueling stations. C_1 and C_2 vary with vehicle size since the energy requirement, purchase cost, and useful life of vehicles vary with vehicle size.

4.1.1. Estimation of fleet size, F

Equation (2) expresses F as the ratio of cycle time, T_C (hr), and scheduled headway, h (hr/veh). h represents the time difference between the arrival of two vehicles at any stop. T_C is twice the one-way travel time between terminal stations and consists of three components: (a) time required to serve on-route requests, T_O (hr), and (b) slack time to serve route deviation requests, T_S (hr), and (c) time required for refuelling in case of ICEV, T_{refuel} (hr) or recharging in case of BEV, T_{Chg} (hr) which may or may not collide with the layover time at terminal stations, T_L (hr). T_L is a fixed time interval inserted in the schedule for drivers' rest or boarding/alighting process.

$$F = \left[\frac{T_C}{h} \right]^+ = \left[\frac{2\{T_O + T_S + \max(T_L, T_{Chg/refuel})\}}{h} \right]^+ \quad (2)$$

T_O includes total riding time, vehicle acceleration and deceleration time, and dwell time for passenger boarding and alighting as given in Eq. (3). T_S represents the slack time allocated to the timetable to accommodate route-deviation requests, also represented as a one-way trip time difference when the route deviations are accommodated in the trip against serving only on-route requests. Thus, N_{RD} in Eq. (4) represents the number of route deviation requests that can be accommodated for a fixed amount of slack time built into the timetable.

$$T_O = \frac{L}{V_R} + \left(\frac{V_R}{a} + t_d \right) 2Ph \quad (3)$$

$$N_{RD} = \frac{T_S}{\varphi} \quad (4)$$

Here, L is the length of the route (km), V_R is the riding speed (km/hr), V_R/a is the time spent in acceleration and deceleration per stopping with an acceleration/deceleration rate a , t_d is per passenger boarding/alighting time, $2Ph$ is the number of stoppings that is assumed to be twice the number of passengers boarded in a vehicle, which holds true in low-demand situations (Kikuchi and Vuchic, 1982) and is discussed in detail in Appendix A.

ϕ in Eq. (5) is the average time required to serve one route deviation request which includes the time required to deviate an average of $W/4$ from and to the fixed route to serve a curb-to-curb stop request for a pickup/drop-off (see Figure 1). The acceleration/deceleration times of the vehicle and the boarding/alighting times of passengers are not separately included in ϕ , as they are already included in Equation (3) for all passengers, regardless of request type, since in the event of insufficient slack time, all passengers will receive service along a fixed route without deviations.

$$\phi = \frac{\left(\frac{W}{4} + \frac{W}{4}\right)}{V_R} = \frac{W}{2V_R} \quad (5)$$

In the case of ICEV, range limitations are not generally a concern since the size of the fuel tank typically allows vehicles to complete all scheduled trips without having to refuel; thus, the time required for refueling, T_{refuel} is zero. Essentially, T_C for ICEV can be expressed as $2(T_O + T_S + T_L)$.

T_{Chg} for opportunity charging estimated using Eq. (6) is the time required to charge a BEV after serving a one-way trip including deadheading and prepositioning time, $T_{\text{preposition}}$. $T_{\text{preposition}}$ is the time required for the charging operation to be initiated and completed including the time required for the bus driver to park and withdraw the vehicle at the charging platform and plug in and plug out the charger. In Equation (2), if T_L is greater than or equal to T_{Chg} , vehicle charging operation is made within a predefined operation time slot T_L ; thus, the charging process, in this case, would not impact the fleet size and introducing additional charging time will result in more idle time in the schedule. Otherwise, fleet size increases as vehicles need to spend additional time at header stations to perform charging operations.

$$T_{\text{Chg}} = \frac{\left[S \left\{ L + N_{RD} \left(\frac{W}{2} \right) \right\} + 2L_D \right] E_C}{B_{\text{Chg}}} + T_{\text{preposition}} \quad (6)$$

Here, E_C is the energy consumption factor (kWh/veh-km), B_{Chg} is the charging speed (kWh/h), and L_D is the deadheading distance. S in Eq. (7) represents the number of trips served before recharging operation and ensures that this number although limited by the battery capacity does not exceed the number of trips served by the ICEV counterpart during the entire day's operation with H service hours.

$$S = \min \left[\frac{E_b (1 - SoC_{\min})}{\left[\left\{ L + N_{RD} \left(\frac{W}{2} \right) \right\} + 2L_D \right] E_C}, \frac{H}{T_O + T_S + T_L} \right] \quad (7)$$

Here, E_b is the battery capacity of the vehicle and SoC_{\min} is the minimum state of charge of the batteries maintained to avoid complete depletion of battery reducing the damage to the energy storage system and consequently, shorter lifetime. SoC_{\min} is defined as the ratio of available to nominal capacity that varies between 0 and 1. Essentially, $E_b \times SoC_{\min}$ is the minimal energy that buses must present at any moment of the service in case of emergency.

4.1.2. Estimation of energy consumption factor, E_C

We have adopted the energy demand model derived by Gallet et al. (2018), which is based on a common longitudinal dynamics model for electric vehicles and incorporates real-world bus route characteristics. E_C between two consecutive vehicle stoppings defined in Eq. (8) consists of two main energy systems: (1) propulsion system (E_{Prop}) and (2) auxiliaries (E_{Aux}). E_{Prop} is the energy demand due to tractive and E_{Aux} is the energy consumed providing auxiliary power for Heating, Ventilating, and Air Conditioning (HVAC), P_{HVAC} and various auxiliary services, P_{others} (such as operating doors, powered steering, lighting, in-vehicle displays, etc.). l is the inter-stop distance and as shown in Eq. (9) is defined as the ratio of total one-way distance travelled and the number of identical stopping phases. Now, as shown in Eq. (8), E_{Prop} for each phase (i.e., inter-stop) has two components (1) energy consumed during start and end consisting of constant acceleration/deceleration with rate ' a ' over distance l_0 estimated as $V_R^2/2a$, (2) energy consumed during riding with constant speed V_R over distance $l-2l_0$. The interaction of traction force components like aerodynamic drag force, rolling friction, grade force, and inertia force in E_{Prop} calculation is derived in Appendix B. P_{aux} in kW is the constant auxiliary power required within the vehicle over the driving duration between two stoppings.

$$E_C = \frac{E_{\text{Prop}} + E_{\text{Aux}}}{l} = \frac{2l_0(Mgf_r) + (l - 2l_0)(Mgf_r + 0.5\rho C_d A_f V_R^2) + P_{\text{aux}} \left(\frac{T_o + T_S}{2Ph + 1} \right)}{l} \quad (8)$$

$$l = \frac{\left\{ L + N_{RD} \left(\frac{W}{2} \right) \right\}}{2Ph + 1} \quad (9)$$

Here, the total mass of vehicle M is the sum of the curb weight M_{curb} and the total mass of the passengers on board with the average weight of the passenger as m_{pass} (i.e., $M = M_{\text{curb}} + Phm_{\text{pass}}$), g is the acceleration due to gravity (m/s^2), f_r is the coefficient of rolling, C_d is the drag co-efficient, ρ is the air density (kg/m^3), and A_f is the vehicle frontal area (m^2).

4.1.3. Estimation of distance travelled by the fleet per unit time, L_F

As shown in Eq. (10), L_F is estimated as the ratio of the length of the roundtrip and service headway as there will be a vehicle that has completed an entire roundtrip with charging at each time headway h .

$$L_F = \frac{2 \left\{ L + N_{RD} \left(\frac{W}{2} \right) \right\} + 2L_D}{h} \quad (10)$$

4.1.4. Estimation of battery capacity on-board, E_b

Opportunity charging requires a battery package of capacity E_b defined in Equation (11) as the product of the number of batteries (N_{batt}) and the nominal capacity of each battery ($E_{b_nominal}$). Due to the installation of charging stations at the end of the route, the number of batteries is estimated as the ratio of the energy required to complete a single one-way trip including the deadheading and the available battery capacity based on the minimum state of charge.

$$E_b = N_{batt} \times E_{b_nominal} = \left[\frac{\left[\left\{ L + N_{RD} \left(\frac{W}{2} \right) \right\} + 2L_D \right] E_C}{E_{b_nominal}(1 - SOC_{min})} \right]^+ \times E_{b_nominal} \quad (11)$$

4.1.5. Estimation of the number of chargers, N_{st}

The number of chargers to be deployed at both ends of the route for opportunity charging is given by twice the ratio of T_{Chg} and h as shown in Equation (12). In the case of opportunity charging, when $T_{Chg} > h$ there will be multiple vehicles demanding the same charging station/outlet; thus, it is required to increase the number of charging stations/platforms to allow multiple vehicles to charge simultaneously. Thus, Equation (12) provides the necessary condition to dispatch vehicles from the initial stop at the defined time headway, h .

$$N_{st} = 2 \left[\frac{T_{Chg}}{h} \right]^+ \quad (12)$$

4.2. User cost

The user cost (C_{UC}) is the sum of the costs of the three equivalent time components, access/egress time, C_{AT} , waiting time, C_{WT} , and in-vehicle time, C_{IT} , estimated in \$/hr given in Equation (13).

$$C_{UC} = C_{AT} + C_{WT} + C_{IT} \quad (13)$$

4.2.1. Access time cost

When requesting a flag stop, passengers must walk/wheel an average vertical distance of $W/4$ from their origin and destination to the fixed route, and curb-to-curb pick-ups/drops involve no walking (see Table 2). Thus, type 1 passengers walk a total of $W/2$ including $W/4$ for access and $W/4$ for egress, and type 2 and type 3 passengers walk $W/4$ for access/egress. Hence, the expected walking time cost can be estimated using Equation (14).

$$C_A = C_5 P \left[\frac{W}{2V_a} \times (\gamma_1) + \frac{W}{4V_a} (\gamma_2 + \gamma_3) \right] \quad (14)$$

where, V_a (km/hr) is the passenger walking speed, and C_5 (\$/pass-hr) is the passenger value of time.

4.2.2. Waiting time cost

The mean waiting time for passengers requesting a flag stop pick-up can be calculated using the value in Table 2 proposed by Ansari Esfeh et al. (2021) and also implemented in Mishra et al. (2023) for low-demand routes characterized by low-frequency service and

Table 2

Values of user time components classified by request type.

Flexibility increases	Type	Pick-up location	Drop-off location	Demand proportion	Access time	Waiting time	In-vehicle time
1	Fixed route	Fixed route	Fixed route	$\gamma_1 = \frac{1}{4}$	$\frac{W}{4V_a} + \frac{W}{4V_a}$	$\left[\frac{1}{2} - \frac{\alpha(1-\beta)}{2} \right] h$	$\frac{T_o + T_s}{2}$
2	Fixed route	Curb-to-curb	Curb-to-curb	$\gamma_2 = \frac{1}{4}$	$\frac{W}{4V_a}$	$\left[\frac{1}{2} - \frac{\alpha(1-\beta)}{2} \right] h$	$\frac{T_o + T_s}{2}$
3	Curb-to-curb	Fixed route	Fixed route	$\gamma_3 = \frac{1}{4}$	$\frac{W}{4V_a}$	0	$\frac{T_o + T_s}{2}$
4	Curb-to-curb	Curb-to-curb	Curb-to-curb	$\gamma_4 = \frac{1}{4}$	0	0	$\frac{T_o + T_s}{2}$

published timetable. Curb-to-curb pickup does not incur any additional waiting time for passengers. The expected value of waiting time can therefore be estimated using Equation (15).

$$C_w = C_s P \left[h \left[\frac{1}{2} - \frac{\alpha(1-\beta)}{2} \right] (\gamma_1 + \gamma_2) \right] \quad (15)$$

where α and β are the proportion of planning passengers and the proportion of planning passengers with fixed arrival times, respectively.

4.2.3. In-vehicle time cost

Similarly, passengers can be dropped off/picked up uniformly anytime in the trip between two terminals. Thus, the average in-vehicle time for passengers is half of the total travel time between the two terminals with the expected value given in Equation (16). In addition, charging time does not affect the in-vehicle time since vehicles will be charged at the terminals during the lay-over time with no passengers onboard.

$$C_I = C_s P \left[\frac{T_o + T_s}{2} \right] (\gamma_1 + \gamma_2 + \gamma_3 + \gamma_4) = C_s P \left[\frac{T_o + T_s}{2} \right] \quad (16)$$

4.3. Environment cost

The emission monetization associated with the circulation of vehicles per unit time can be estimated by Equation (17), considering the total distance run by the whole fleet per unit time. It is considered that BEVs do not present any pollutant contribution.

$$C_{ENV} = L_F \times \sum_{x \in X} Z_x \epsilon_x \quad (17)$$

Here, ϵ_x a proxy parameter to monetize the effect of producing one unit of pollutant $X \in$ (in \$/gm of pollutant X) and Z_x is the mass of local pollutant x ($x \in X$) per kilometer run (gm/veh-km).

5. Problem optimization and solution technique

The optimal equilibrium between the costs for the transit operator, transit user, and the environment is achieved by minimization of the total cost (C_{TC}) considering two continuous decision variables: (a) service headway (h) and slack time (T_s). Equation (18) states the mathematical formulation of the optimization problem, C_{TC} expressed in units of \$/hour is the sum of the operator cost (C_{OC}), user cost (C_{UC}), and environment cost (C_{ENV}). The problem constraints ensure that decision variables must take positive values with thresholds defined by transit agencies and the vehicle occupancy must be equal to or lower than the vehicle capacity (C). The optimal solution is identified by examining the entire solution space (i.e., different combinations of the decision variable value) with simple enumeration (i.e., brute force) considering different vehicle technologies and types as discussed in section 3. Essentially, the six scenarios evaluated include (1) ICEV-Minivan, (2) ICEV-Van, (3) ICEV-Minibus, (4) BEV-Minivan, (5) BEV-Van, (6) BEV-Minibus.

$$\min_{h, T_s} C_{TC} = C_{OC} + C_{UC} + C_{ENV} \quad (18)$$

subject to

$$h_{min} \leq h \leq \min \left(\frac{C}{P}, h_p \right) \quad (19a)$$

$$0 \leq T_s \leq 2Ph\varphi \quad (19b)$$

Equation (19a) depicts that h is constrained by a minimum and maximum service headway. Literature consensus that for a low-demand route characterized by low-frequency service, the minimum headway can be set to 10 min (Ansari Esfeh et al., 2021). While the maximum headway is governed by the minimum desired level of service set through policy headway, h_p , and vehicle capacity. As shown in Equation (19b), T_s should vary between 0 and a maximum value based on observed demand ensuring that slack time cannot exceed the time required to provide route deviations for both pick-up and drop-off for all passengers in the system.

To enumerate feasible solution sets for (h, T_s) for each of the six scenarios, the brute force method is used to identify feasible solutions from a grid of possible solutions that satisfy the constraints of Equations (19a)-(19b). The two-dimensional grid representing possible combinations of h and T_s is defined over the minimum and maximum values indicated in 19(a) and 19(b), respectively, at an enumeration interval pace of one minute for each variable. The total cost for all feasible solutions is calculated using Equation (18) to determine the optimal combination of h and T_s that corresponds to the minimum total cost for each scenario. Furthermore, we report the optimal vehicle size and technology combination that results in the minimum average total cost, averaged across all feasible solutions for the corresponding scenarios.

6. Results and discussion

6.1. Case study

The optimization models developed are applied to a bus route with low passenger demand in Regina, Canada. The primary mode of public transportation in Regina is bus transit, with 118 buses operating on 20 routes during the weekdays, but fewer routes on Saturdays and Sundays. A report by CUTA (2015) suggests that Regina Transit serves an average ridership of 25 pass/veh-hr with an average revenue-to-cost ratio (R/C) of only 26.27 %; while the remaining 73.73 % of the cost is subsidized by non-users. On analyzing the ridership and operation data obtained from Regina Transit for 2015 we found that routes 6, 14, 15, 16, 17, 21, and 40 are underperforming routes (i.e., R/C < 26.27 %) as shown in Fig. 2. For case study analysis we randomly selected Route 6 attributed to low ridership (p) of 9 pass/hr, R/C of 15.3 %, and the high operating cost of \$10.84/pass. The first step in solving the optimization problem involves defining a base case study based on the input parameters of the model described in Appendix C. The results of optimization are presented in the following sections. In Equation (19a), the constraint limits h between [10, 46] minutes for the minivan and [10, 60] minutes for the standard van and minibus, while in Equation (19b), the constraint limits T_S between [0, 11] minutes for the minivan and [0, 15] minutes for the standard van and minibus. Constraints 19(a) and 19(b) results in 284 feasible solution sets of (h, T_S) for the minivan and 484 feasible solution sets of (h, T_S) for the standard van and minibus. The deriving of the above number of feasible solution sets and estimation of corresponding operator cost, user cost, and total cost using the enumeration technique takes an average of 63 s in the following running environment: (a) software: R programming, (b) processor: 3.30 GHz Intel (R) Xeon(R) E-2136 CPU, (c) RAM: 32.0 GB, and (d) system type: 64-bit operating system. A list of definitions and notations of important parameters is included in Table D1 in Appendix D.

6.2. Comparison of costs for different vehicle technologies

Fig. 3 summarizes the average of the operator, user, and total cost components considering different SFT vehicle technologies in Route 6. Despite the charging strategy, the average operating cost (C_{OC}) with BEV is higher than the corresponding cost to ICEV counterparts and this cost increases with vehicle size with a rate higher in the case of ICEV than BEV. In the BEV, the average operating cost increased by 2.8 %, 7.6 %, and 13.1 % from ICEV counterpart for minivan, standard van, and minibus, respectively. It is observed that for both ICEVs and BEVs, the standard van has the lowest average fleet cost. ICEV fleet costs are lower for minibuses than minivans, while BEV fleet costs are lower for minivans than minibuses. Service headway, h range suggests greater average fleet size for the minivan and the same for a standard van and minibus. However, this difference in fleet costs is a result of the increase in unit temporal costs with vehicle size, which is more significant for BEVs than for ICEVs. Additionally, the average energy consumption factor (E_C) increases with vehicle size with values 0.07kWh/km, 0.17kWh/km, and 0.26kWh/km for BEV based minivan, van, and minibus, respectively, contributed by increasing gross vehicle weight and number of stoppings. Consequently, given that each vehicle is equipped with a 25kWh battery pack, and the minimum required state of charge is constrained to 0.2, the average number of one-way trips that can be served with 80 % charging decreases with vehicle size with 17, 7, and 4 trips, respectively, for minivans, vans, and minibuses. For a given layover time (T_L) of 5 min, T_L exceeds the required charging time (T_{Chg}) for all instances varying from 2 to 2.6 min; therefore, charging of a BEV can be accomplished within a predefined operation time slot without changing the existing schedule if the transit agency wishes to transition from ICEV to BEV. The average energy costs increase with vehicle size and for each vehicle size, the cost drops approximately by 70 % from ICEV to BEV. It is estimated that the average range of a minivan BEV is 277 km, while that of a minibus BEV is 68 km, with battery costs remaining the same regardless of vehicle size. Finally, the infrastructure costs are only a function of vehicle technology and are significantly higher for BEV (i.e., \$8/hr) than ICEV (i.e., \$0.14/hr). Interestingly, if infrastructure cost is excluded similar to results reported by Estrada et al. (2021), BEV always outperforms ICEV for all vehicle sizes; thus, the potential savings in energy cost in favor of BEV was neutralized by the current expensive cost of installing fast chargers. Similarly, Tirachini and Antoniou (2020) suggested that the operator cost of BEV comprising of vehicle capital costs, driver costs, and running costs, (e.g., energy consumption and maintenance) increases with vehicle size and the total operator cost for BEV car, van, and minibus are €18.9/veh-h, €20/veh-h, and €28.7/veh-h. On analyzing user cost (C_{UC}) it is observed that the average access costs are insensitive to vehicle size and technology, vehicle capacity determines the maximum headway, which in turn affects average waiting and in-vehicle costs with the lowest values observed for minivans for a maximum h of 47 min. In addition, there is no environmental cost (C_{ENV}) associated with BEV while this cost exists and increases with vehicle size for an ICEV. Finally, in terms of the total cost (C_{TC}), a minivan ICEV outperforms all other scenarios and for standard van and minibus, BEV technology offers lower total cost than ICEV with the total cost increasing with vehicle size irrespective of technology.

6.3. Variation of cost components with h and T_S

In this section, we establish general relationships between CTC, COC, and CUC with decision variables using descriptive analysis plots for all scenarios in Figs. 4 and 5. Figs. 4 and 5 demonstrate that the CTC is non-linearly related to h and T_S . The shape of the curve between CTC and h is a U-shaped curve suggesting that mid-range headway values appear to be optimal, whereas the curve between CTC and T_S shows an approximate linearly increasing trend suggesting that low T_S values minimize CTC. Additionally, the range of CTC values decreases with T_S and increases with h , since a higher service interval/headway indicates more passengers in the system, resulting in more slack time required to accommodate route deviations; thus, the upper limit of T_S values increases with h . According to Fig. 4, the rate of increase in CTC with h is higher for ICEVs than for BEVs at values of h less than the optimal value, whereas the

opposite holds for values of h greater than the optimal value. Fig. 5 suggests that for $TS < 5$ min, the variation in CTC with TS is more with respect to ICEVs than BEVs whereas, for $TS > 5$ min, the variation is not significant with respect to vehicle technology. As a result, SFT with BEV-based system is more preferred when the optimal values of h and TS are in the lower range with $h < 30$ min and $TS < 5$ min (i.e., comparatively high frequency service with fewer curb-to-curb services) since the variation in CTC is smaller than ICEV. Similarly, for $h > 30$ min and $TS > 5$ min, SFT with ICEV-based system proves more beneficial. Additionally, Fig. 5 suggests that for a given h , as TS increases CTC increases, and for a given TS , as h increases CTC increases for low and high-value ranges, confirming the U-shaped and linear relationship of CTC with h and TS . Additionally, from Fig. 5, graphically we can conclude that the optimal range of h is between 20 and 30 min and TS is between 0 and 5 min. Thus, observations from Figs. 3, 4, and 5 suggest that operating SFT with BEV with $h < 30$ min and $TS < 5$ min is the optimal configuration for route 6.

Using Fig. 4 (g), 4 (h), 5 (g), and 5 (h), we will examine the relationship of the operator (C_{OC}) and user cost (C_{UC}) with h and TS for minivans BEVs, however, the relationship derived holds for all other scenarios as well. As the figure suggests, C_{OC} is inversely related to h and TS , while C_{UC} is directly related to h and TS , while linear relationship approximations are better established with h than with TS . With respect to C_{OC} , an increase in h results in a reduction in the required fleet size, thereby reducing the battery cost and the distance that the fleet travels per unit of time, contributing to lower energy costs. Furthermore, as TS increases, round trip distance increases, which increases energy costs and battery costs; however, high TS values are only associated with high h values, which reduces fleet size, explaining the inverse relationship between C_{OC} with TS . Infrastructure costs, however, are not affected by h since the required charging time is always less than the headway. In addition, for C_{UC} , access/egress time, C_A , is not determined by h and TS ; however, waiting time, C_W , is only positively related to h , while in-vehicle time, C_I , is positively related as higher h and TS increases the one-way travel time. Estrada et al. (2021) also demonstrated that for flexible and fixed-route service with diesel and battery-operated vehicles, the operator and user costs usually present a strictly decreasing and increasing behavior, respectively regarding h . For diesel-based flexible-route systems, Alshalalfah (2009) estimated that fleet size would increase as a function of the ratio of slack time to original headway, similar to Eq. (2). Yoon et al. (2022) suggested that compliance with timetables with slack time could result in longer travel times since there will be longer waits and in-vehicle time. TS , however, affects wait time only when the fleet size is fixed, since TS increases the round-trip time, which implies higher headway values; therefore, longer waits.

6.4. Sensitivity analysis

6.4.1. Charging speed, B_{Chg}

This section analyses the impact of the variation in charging rate at the end stop location on the fleet cost and charging infrastructure cost; thus, total cost, where the charging rate takes values between [0.5, 7.5] kWh/min as shown in Fig. 7 and the difference in costs from base case scenario is presented in Table 3. In contrast to the base case scenario where the charging rate is 7.5 kWh/min, when charging rates are varied, BEVs are most affected, resulting in a difference between 0.3 and 16.8 % in total costs. In the base case scenario, the average T_{Chg} for a minivan BEV is 2.3 min; however, at the lowest charging rate of 0.5 kWh/min, it is 39 min. Thus, since the layover time of 5 min is less than the average T_{Chg} , the fleet size requirements increase and vary between 3 and 13 vehicles instead of 2–6 vehicles. Also, the number of chargers varies between 2 and 8 compared to 2 chargers in the base case scenario. Thus, the average total costs decrease continuously as B_{Chg} increases from 0.5 to 3 kWh/min since the charging infrastructure and fleet size requirements drop, and for charging speeds ≥ 4.5 kWh/min the average total costs increase as the unit charging facility cost increases proportionally with charging rate (i.e., both cost and charging rate increase at the same rate). Further analysis indicates that when operating minivan BEVs equipped with 25 kWh battery packs and stations with 0.5 kWh/min charging rate, increasing the minimum required state of charge (SoC) from 20 % to 50 % reduces the total cost by 7.13 % due to the reduction in charging time, resulting in a reduction in fleet size and charging infrastructure requirements. Further, when operating minivan BEVs with 0.5 kWh/min charging rate, reducing battery size from 25 kWh to 10 kWh with 20 % minimum SoC results in an 11.3 % reduction in total cost, as both battery cost and charging time are reduced. To effectively reduce the total system cost, a tradeoff between battery capacity/battery cost and the cost of the charging station can be considered. A study conducted by Sung et al. (2022) also supports such a conclusion.

Assuming a linear relationship between the unit charging facility cost and the charging rate, in this study, the unit charging facility cost increases from \$0.533/charger-hr for slow charging speed of 0.5 kWh/min to \$8.008/charger-hr for fast charging speed of 7.5 kWh/min, which is a 15-fold increase. Liu et al. (2019) also assumed a linear relationship between charger cost and power levels with a 90-kW plug-in depot charger costing 40,000 USD with fixed cost of \$13,000 and variable cost of \$300/kW while it costs \$500,000 to deploy a 500-kW on-route overhead fast charging station with fixed and variable costs at \$150,000 and \$700/kW, respectively (i.e., nearly 12.5 times). However, the infrastructure cost may increase non-linearly with grid upgrade required for fast chargers with high

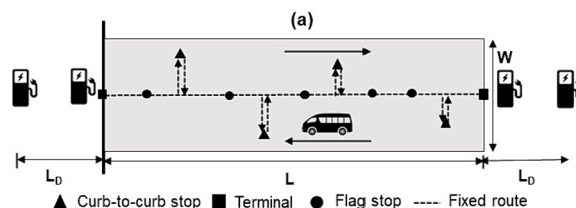


Fig. 1. A schematic representation of route-deviation operating policy with charging scheme.

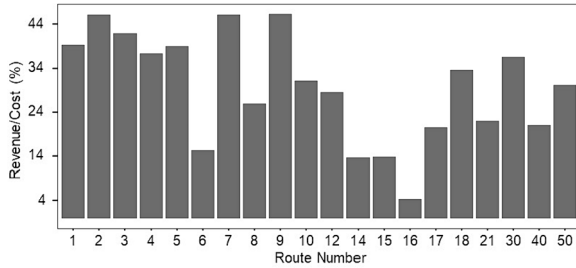


Fig. 2. Performance indicators for Regina bus routes.

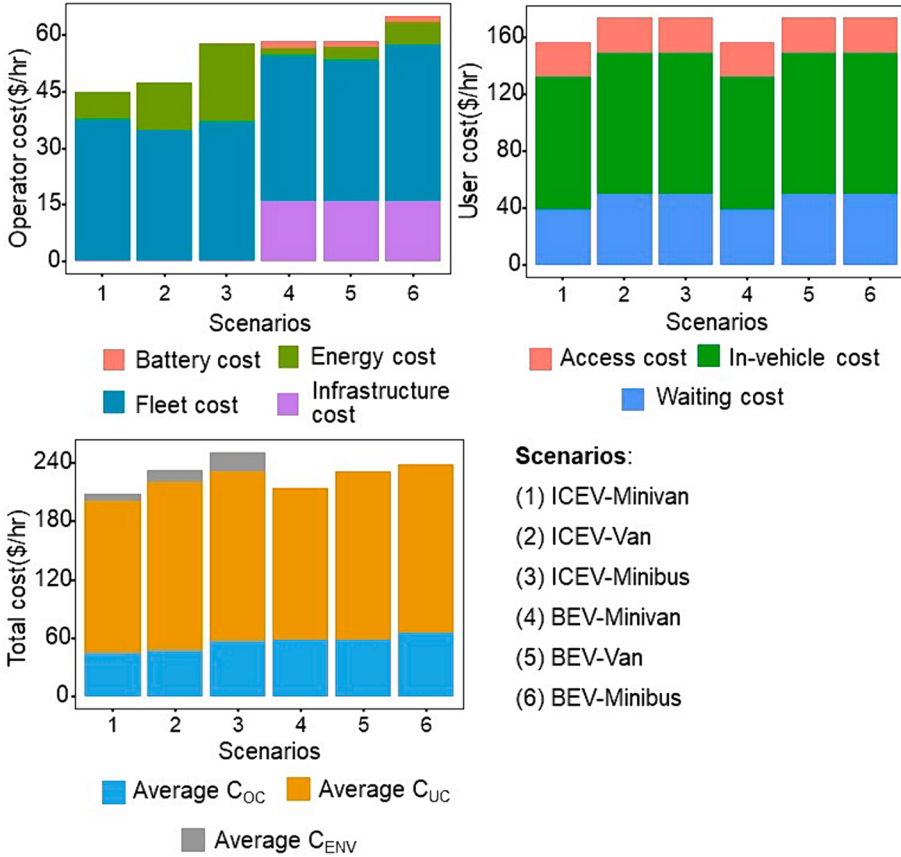


Fig. 3. Average of total cost and cost components incurred in the provision of ICEV, and BEV-based SFT service.

power involved unless installation is done at higher voltage grid levels. Study by [Schroeder and Traber \(2012\)](#) suggests that as charging times shorten the cost of charging infrastructure increases disproportionately when evaluating charging levels from 1000EUR for 3.6 kW ‘Level II’ AC chargers to 125000EUR for 250 kW ‘Super-fast’ DC chargers (i.e., 125-fold increase).

6.4.2. Hourly demand, P

In their initial feasibility analysis along this route, [Mishra et al. \(2020\)](#) recommended regular bus transit over SFT when demand exceeds 27 pass/hr; thus, in this analysis, we varied the demand over a range of 5, 15, and 25 pass/hr. [Fig. 8](#) illustrates that when the demand for service increases, the average total cost, C_{TC} , increases regardless of vehicle size and technology. For each technology, when demand increases from 5 to 15 pass/hr, standard vans experience the greatest increase in C_{TC} , followed by minibuses and minivans; however, when demand increases from 15 to 25 pass/hr, minibuses experience the greatest increase in C_{TC} followed by minivans and standard vans. In addition, when demand increases from 5 to 15 pass/hr, the average change in C_{TC} considering all scenarios is 136.2 % while for the increase in demand from 15 to 25 pass/hr, the change is 55.8 %. Concerning technology, the change in total costs with demand is comparatively more significant for BEV than ICEV. Interestingly, minivan ICEV outperforms all other scenarios when demand levels are 5 pass/hr and 15 pass/hr, and for these demand levels ICEV minivan and standard van offer lower

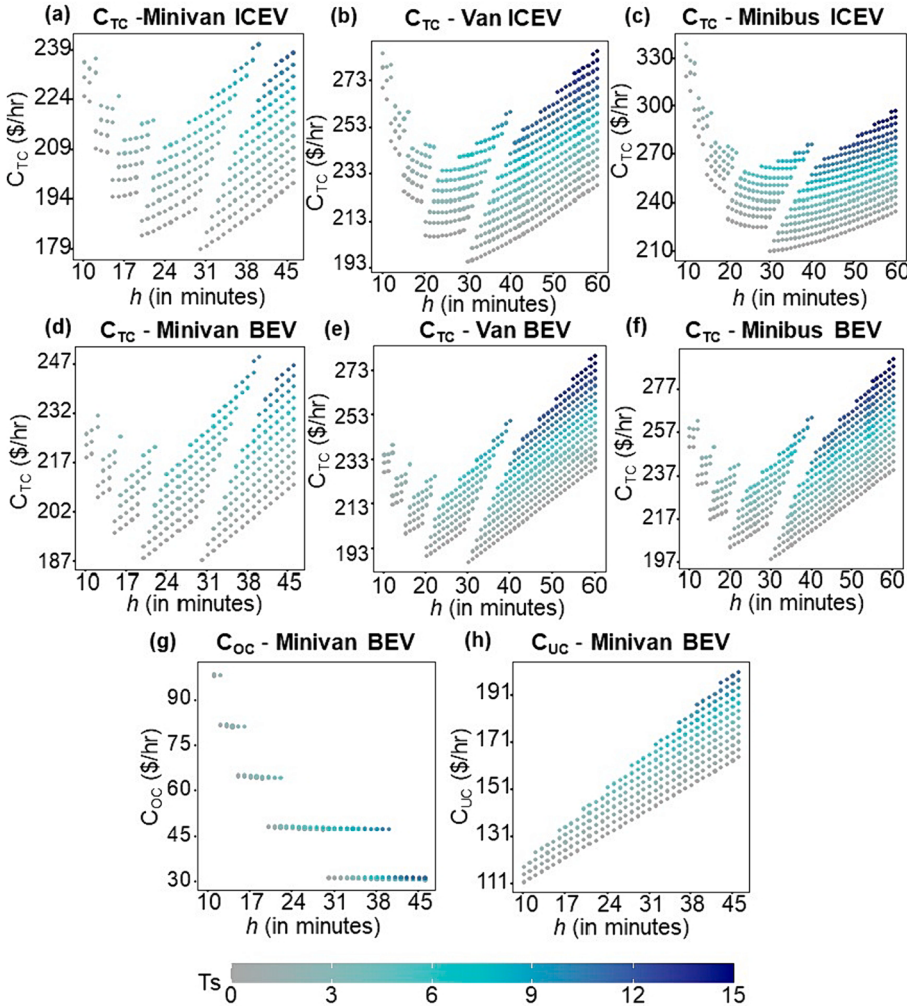


Fig. 4. Variation of the total cost, operator cost, and user cost with h color-coded by T_s .

C_{TC} than their BEV counterparts. However, when demand increases to 25 pass/hr, minivan BEV outperforms all other scenarios and irrespective of vehicle size BEV offers lower C_{TC} than ICEV counterparts. Also, for all levels of demand, minibuses with BEV technology have lower C_{TC} than ICEV technology. Further, at all levels of demand and technology, minivans are more economical than standard vans and minibuses. The results are consistent with those reported by Estrada et al. (2021) suggesting that for low to medium demand densities (i.e., 3 to 92 pass/km²-h), flexible service operated by electric cars with a capacity of 4 pass/veh minimizes the total cost (user and operator cost), followed by diesel-based cars. Transit planners can use this analysis to determine the optimal vehicle size and technology for SFT operation, based on the observed temporal distribution of passenger demand along a route, which typically includes peak and off-peak periods. For example, this analysis suggests that small capacity minivans or standard vans ICEVs could be used during peak periods when demand for service is high, while small capacity BEVs could be used during off-peak times.

Furthermore, from Equation 19(a), it is observed that upper limit of headway decreases with demand and is governed by policy headway for vehicles with larger capacity. In addition to reducing wait times, the decrease in headway increases fleet size requirements and operator costs. Similarly, from Equation 19(b), the upper limit of slack time increases with demand and vehicle capacity, and as slack time increases, the number of route deviations increases, resulting in longer vehicle travel times. As a result, higher slack time increases user in-vehicle time and fleet size. As discussed in section 6.3, the rate of increase in operating costs with regard to decreases in headway is greater than the rate of decrease in waiting time costs and the increase in in-vehicle time costs due to an increase in slack time, leading to an increase in total costs with demand for all scenarios, as illustrated in Table 3.

6.4.3. Battery size and state of the charge

Fig. 9 and Table 3 illustrate that as battery size increases the total cost increases by 0.6 % to 4 %. For a given battery size, if the minimum required state of charge (SoC) increases from 20 % to 50 %, the total cost may decrease varying between 0 % and -1.55 %. For a standard van with a 100kWh battery, as the minimum SoC increases from 20 % to 50 %, the amount of charging required after

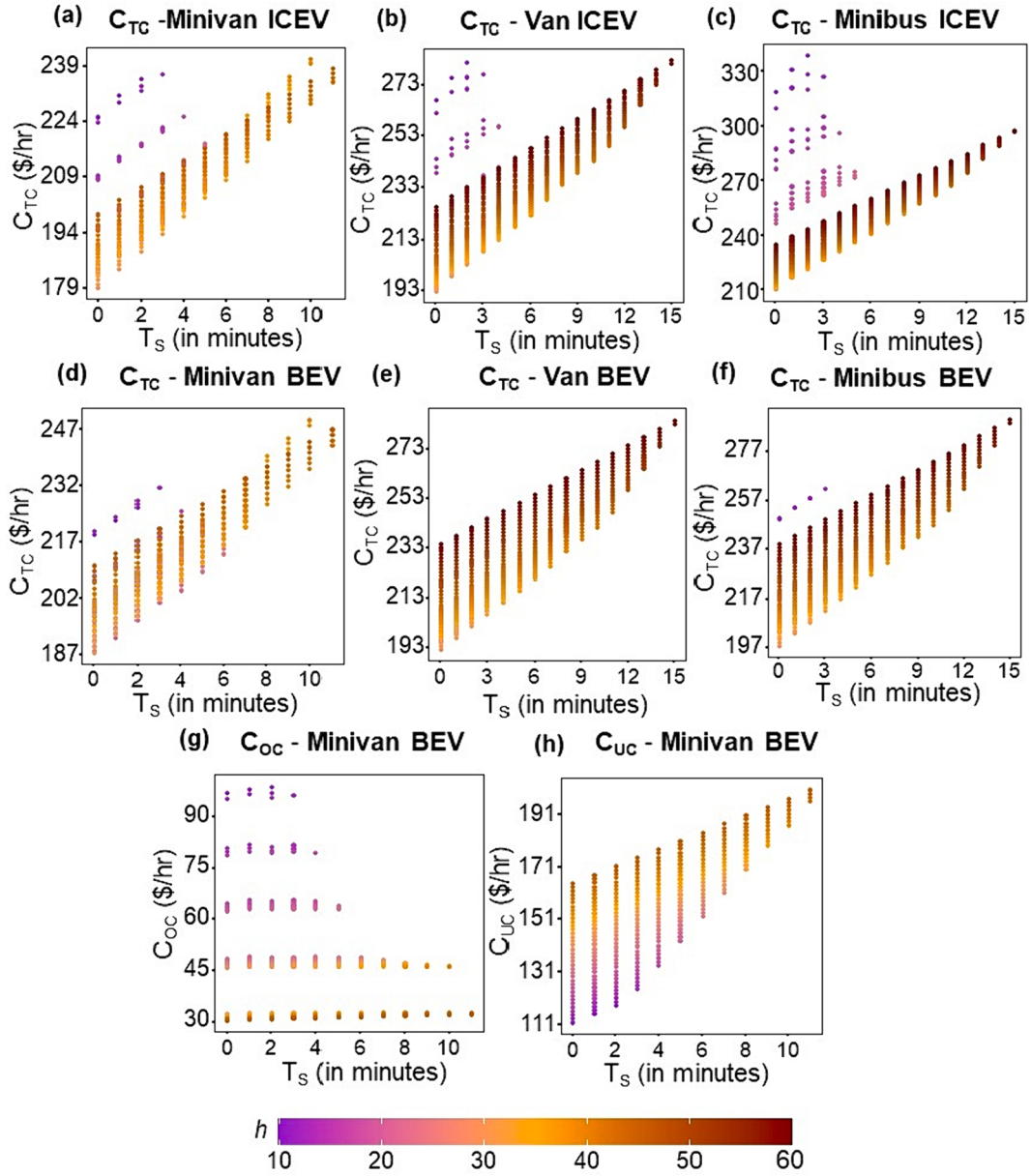


Fig. 5. Variation of total cost, operator cost, and user cost with T_S color coded by h .

completing the maximum number of trips decreases; thus, average T_{Ch} decreases from 8 to 6.5 min, so fleet size decreases, resulting in a 1.55 % decrease in total cost due to fleet and battery costs. Additionally, for any given SoC, as the battery size increases, the number of one-way trips will increase before recharging; this will result in a greater charging time; thus, larger fleet size and higher total costs. Moreover, it is important to note that battery size has a negligible impact on the total cost compared to charging speed and demand, so modifying this parameter would have little impact on the total cost.

6.4.4. L/W ratio

In addition to the $L = 13$ km, $W = 1$ km base scenario ($L/W = 13$), the total cost is estimated for $L = 6.5$ km, $W = 2$ km ($L/W = 3.25$) to analyze the effects of a lower L/W ratio representing a less stretched area and study the influence of service area shape on SFT operation (refer Figure 1). Assumption C in section 3 states that the demand is assumed to be uniformly distributed over the area; since the area remains the same, the hourly demand for service area with $L = 6.5$ km, $W = 2$ km ($L/W = 3.25$) remains unchanged from the base scenario. The results indicate that the average total cost increases for $L/W = 3.25$ in comparison to $L/W = 13$, and the percentage increase for BEVs is more significant than for ICEVs while decreasing as vehicle size increases. Specifically, the percentage increase in CTC ranges from 8.3 to 3.1 % for ICEVs and 10 % to 8.5 % for BEVs. For all scenarios, the user cost increases by nearly 13 % as access

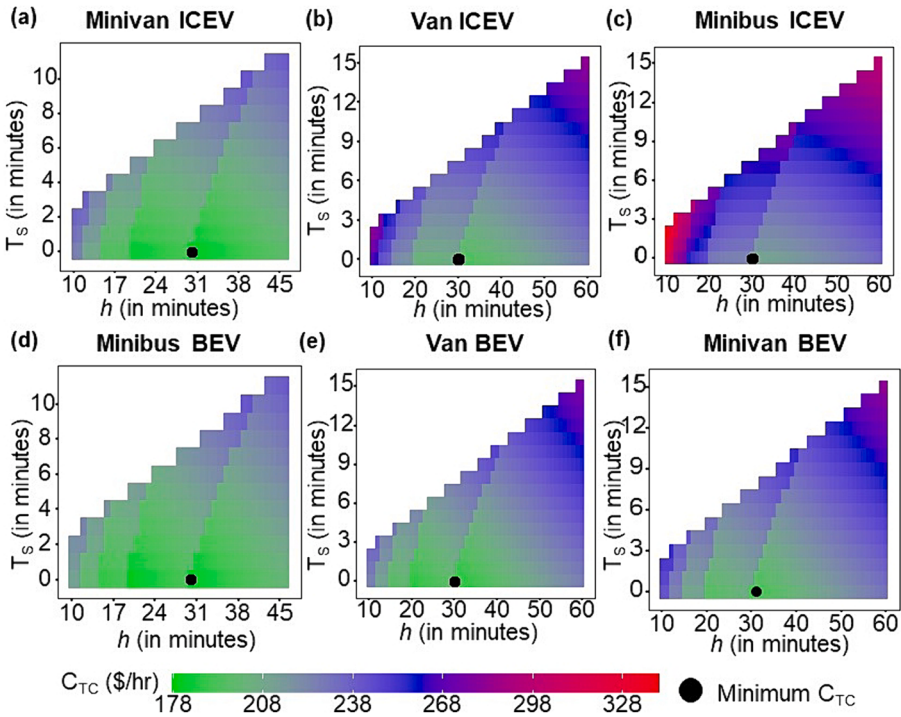


Fig. 6. Heatmap illustrating the variation of the total cost with h and T_S for all scenarios.

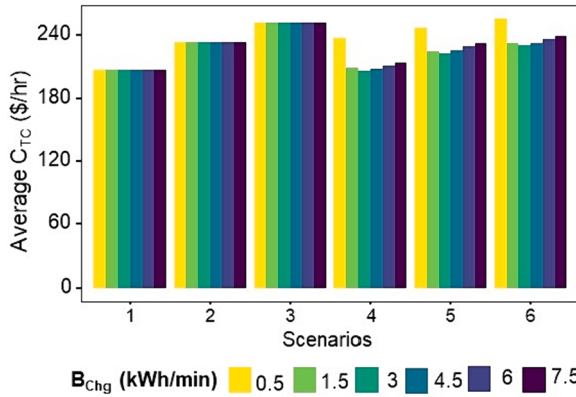


Fig. 7. Sensitivity analysis of the total cost based on the charging rate.

and egress time to stations for passengers with flag stops increases with the decrease in L/W ratio. Conversely, for low L/W ratios, the distance travelled by the fleet decreases, resulting in lower energy requirements and, consequently, lower operator and environmental costs. The decrease in operator costs is, however, greater for ICEVs than BEVs and significant for large vehicle sizes, ranging from 6.5 % to 14.4 % for ICEVs and 1.5 to 3.7 % for BEVs.

6.5. Summarizing sensitivity analysis and ranking of scenarios

Table 3 summarizes the results of the sensitivity analysis, which demonstrate that the total cost of SFT is most sensitive to changes in demand regardless of the vehicle technology or size followed by charging speed (B_{Chg}), service area size (L/W ratio), and available battery capacity. Additionally, it is observed that BEV based SFT is more sensitive to L/W ratio than ICEV counterparts and sensitivity of cost to L/W ratio and B_{Chg} decreases with increase vehicle size. Table 4 summarizes the ranking of scenarios and indicates the sum of the rankings for each scenario. It appears that when all factors are considered, including the level of demand, charging speed, battery size, service area size, and powertrain technology, minivans are more economical than standard vans and minibuses. In terms of vehicle technology, ICEV minivans and vans outperform their BEV counterparts in most scenarios, while for minibuses, BEVs are more

Table 3
Summarizing sensitivity analysis results.

	Average C _{TC} for base case (\$/hr)	Percentage change in average C _{TC} compared to base case														L/W ratio	
		B _{Chg} (kWh/min)					P (Pass/hr)			E _{b,nominal} (kWh), SoC							
		0.5	1.5	3	4.5	6	5	15	25	25	50	50	75	75	100	100	
1	208.1	0.0	0.0	0.0	0.0	0.0	-34.9	74.1	85.4	0.0	0.0	0.0	0.0	0.0	0.0	8.3	
2	233.2	0.0	0.0	0.0	0.0	0.0	-35.9	93.7	84.9	0.0	0.0	0.0	0.0	0.0	0.0	5.9	
3	251.7	0.0	0.0	0.0	0.0	0.0	-33.7	85.1	105.1	0.0	0.0	0.0	0.0	0.0	0.0	3.1	
4	214.9	16.8	3.7	0.7	0.0	0.0	-32.8	66.2	81.3	0.0	0.8	1.0	1.6	1.6	2.4	2.4	10.0
5	232.2	12.6	2.3	0.3	0.0	0.0	-35.6	92.2	82.0	0.0	0.7	0.7	1.3	2.3	2.4	2.9	9.0
6	238.8	13.0	2.2	0.3	0.0	0.0	-34.7	88.8	107.2	0.0	0.6	0.7	1.3	2.3	2.4	4.0	8.5

Scenarios: (1) ICEV-Minivan, (2) ICEV-Van, (3) ICEV-Minibus, (4) BEV-Minivan, (5) BEV-Van, (6) BEV-Minibus

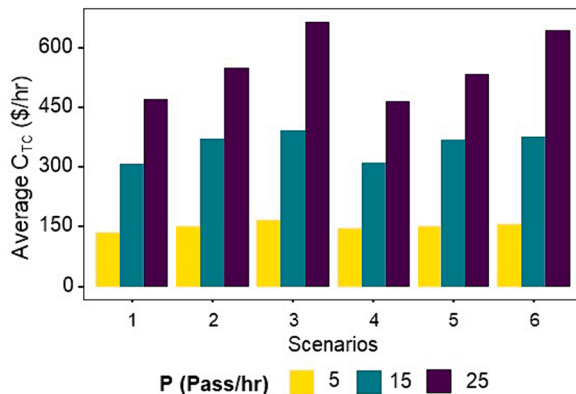


Fig. 8. Sensitivity analysis of the total cost based on hourly demand.

Table 4

Ranking of scenarios.

Base case	B_{Chg} (kWh/min)					P (Pass/hr)			$E_{\text{b,nominal}}$ (kWh), SoC							L/W ratio	Sum of ranks		
	0.5	1.5	3	4.5	6	5	15	25	0.5	0.5	0.2	0.5	0.2	0.5	0.2				
1	1	1	1	2	1	1	1	2	1	1	1	1	1	1	1	1	19		
2	4	2	5	5	5	4	3	4	4	4	3	3	3	3	3	3	61		
3	6	6	6	6	5	6	6	6	6	6	6	6	6	6	6	5	100		
4	2	2	1	2	2	3	2	2	1	2	2	2	2	2	2	2	33		
5	3	3	3	3	3	4	4	3	3	3	4	4	4	4	4	4	60		
6	5	4	4	4	5	6	5	5	5	5	5	5	5	5	5	6	84		

Scenarios: (1) ICEV-Minivan, (2) ICEV-Van, (3) ICEV-Minibus, (4) BEV-Minivan, (5) BEV-Van, (6) BEV-Minibus

economical than ICEVs under most circumstances.

6.6. Impact of weather conditions

The study model is examined at various weather conditions, where the external temperature ranges between -40°C and 40°C , which represent the extreme temperatures encountered throughout the year in parts of Canada. Assuming that passenger load along low demand routes will have a negligible impact on auxiliary power (P_{aux}) and auxiliary power used for secondary auxiliary services (such as operating doors, powered steering, lighting, and in-vehicle displays), P_{others} remains constant regardless of the weather. However, auxiliary power consumption for HVAC (P_{HVAC}) is the highest during extreme weather conditions due to the high thermal load and is comparable to the energy consumption of the propulsion system (E_{prop}). Based on the data published by Basma et al. (2020), it has been determined that P_{aux} is influenced by external temperatures; an approximation function has been developed using this data

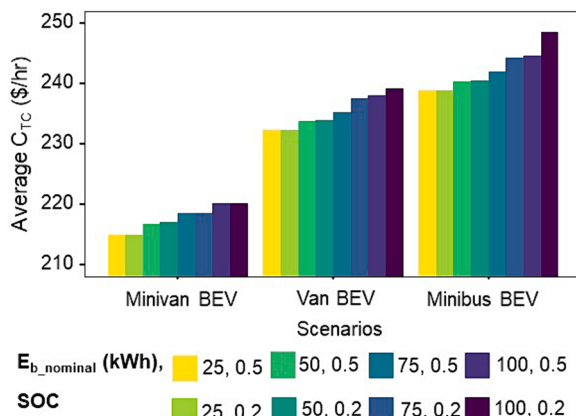


Fig. 9. Sensitivity analysis of the total cost based on battery size and SoC.

in Hjelkrem et al. (2021) as shown in Equation (20) for a 50-seat passenger bus. In this study, equation (20) is used to estimate the P_{HVAC} shown in Fig. 10, and the values are estimated for the vehicle types based on the assumption that P_{HVAC} is linearly related to vehicle size. Results suggest that P_{HVAC} demand increases significantly for extreme weather conditions, specifically for low temperatures during winter.

$$P_{HVAC}(T) = 0.0264T^2 - 1.046T + 11.3 \quad (20)$$

Here, P_{HVAC} is the auxiliary power consumption for HVAC in kW, and T is the temperature in degrees Celsius.

During extreme weather conditions, such as snow, ice, or sleet that are common in parts of Canada during the winter, using a wheelchair or walking to the bus stop can cause significant discomfort or pose a safety risk. We replicated this scenario by reducing walking/wheeling speed, vehicle riding speed, and increasing the proportion of passengers requesting curb-to-curb service for both pickup and drop-off and auxiliary power requirements as shown in Table 5. In cases of extremely low temperatures of $-30/-40^{\circ}\text{C}$, the travel distance increases for higher values of h and T_S ; therefore, the energy required to complete one trip increases; thus, the battery requirement increases for these conditions; thus, increasing the operating cost by only 0.9 % as the charging time does not increase significantly. At a commonly observed temperature of -20°C in Regina during winters, it is observed that although the number of trips completed before recharging decreases, the fleet size remains unaffected as the average charging time for all instances increased from 2 to 2.6 min to 2.8–4.2 min, which is less than the given layover time (T_L) of 5 min. Thus, the operator cost remains unchanged at -20°C ; however, the user cost increases by nearly 2 times for all instances, and the ranking remains unchanged from the base case scenario. Furthermore, it has been observed that significant improvements in operator costs are not observed if the charging rate drops, as the increase in fleet size due to the increase in charging time is compensated for in most cases, by a reduction in infrastructure costs.

7. Conclusion

This paper is aimed at analyzing the effect of the additional requirements of battery electric vehicles (BEVs) for the operation of Semi-flexible transit (SFT) services along low-demand bus routes, considering different headways (h) and slack time (T_S). The analytical models developed are used to provide a detailed estimation of the total costs incurred, including operator, user, and environmental costs, allowing a comparison with conventional vehicle technology: internal combustion engines (ICEV), and comparing three vehicle sizes: minivans (7-seaters), standard vans (15-seaters), and minibuses (25-seaters). The application of the study methodology is demonstrated for a low-demand bus route in Regina, Canada.

The main contributions of this study are as follows:

In terms of overall cost, a minivan with an internal combustion engine (ICEV) was found to be more cost-effective than all other scenarios, as the potential savings in energy cost with battery electric vehicles (BEV) were offset by the present high cost of installing fast chargers. These findings remained consistent when demand levels were 5 and 15 passengers/hour. However, when demand increased to 25 passengers/hour, the minivan BEV was more cost-effective because the savings in energy costs outweighed the infrastructure costs.

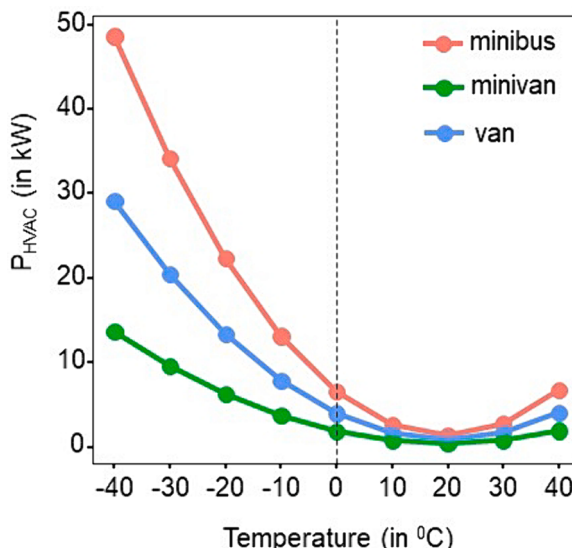


Fig. 10. P_{HVAC} at different external temperatures.

Table 5

System characteristics based on weather conditions.

Weather condition	T °C	V_R km/hr	V_a km/hr	γ_1	γ_2	γ_3	γ_4	P_{aux} kWh
Case 1: Winter	-20	15	0.5	0	0	0	1	Minibus: 22.31, Van: 13.42, Minivan: 6.20
Case 2: Normal	+15	35	4	0.25	0.25	0.25	0.25	Minibus: 2.65, Van: 1.60, Minivan: 0.27

The study found that at all levels of demand, charging speed, battery size, and powertrain technology, minivans were more economical than standard vans and minibuses. Additionally, extreme weather conditions increase user costs significantly and the effect on operator costs is minimum owing to the fast-charging facility.

The study emphasized the importance of carefully considering the choice of headway (h) and slack time (T_S) in SFT operations. Results suggest that SFT with BEV is economically more stable when the optimal values of h and T_S are in the lower range with $h < 30$ min and $T_S < 5$ min while for a higher range of optimal values, SFT with ICEV-based system proves more economically stable.

The study also highlighted that the electrification of SFT services may have a positive impact in terms of reducing operational costs and emissions. However, it is important for transit agencies to carefully evaluate the costs and benefits of electrification, considering factors such as charging infrastructure and vehicle size, before making the decision to adopt electric vehicles for SFT services. Additionally, the study provides insights on how to optimize the headway and slack time in SFT operation which will help the agencies to make more efficient and effective service plans. Limitations of results come from the assumptions of the simplified system configuration like rectangular service area and uniform distribution of demand. Nevertheless, these assumptions allowed us to derive a closed-form analytical expression for SFT total cost, which can aid practitioners in making decisions at the planning level. Future extensions will analyze the effect of irregular service area and stochasticity in demand and service, assumptions related to estimation of unit costs and energy consumption, and alternative solution algorithms.

CRediT authorship contribution statement

Sushreeta Mishra: Conceptualization, Formal analysis, Methodology, Software, Visualization, Writing – original draft. **Babak Mehran:** Conceptualization, Methodology, Supervision, Writing – review & editing.

Declaration of competing interest

The authors declare that they have no known competing financial interests or personal relationships that could have appeared to influence the work reported in this paper.

Data availability

Data will be made available on request.

Appendix A

Probability of stopping along a low demand bus route.

Along a low demand route, an on-call stop policy is practiced (Kikuchi and Vuchic, 1982), and the general expression for the expected number of stops, $E(s)$ along a route is given in Equation (A1). Transit stopping is assumed to follow a binomial distribution, and passenger arrival is Poisson distributed at a stop. The binomial distribution assumes equal passenger demand for boarding/alighting (λ) at any stop location along a route.

$$E(s) = n \left[1 - e^{(-\lambda)} \right] = n \left[1 - e^{\left(-\frac{2ph}{n} \right)} \right] \quad (\text{A1})$$

$$E(s) = \begin{cases} n, & \text{if } ph \rightarrow \infty \\ 2ph, & \text{if } ph < n \end{cases} \quad (\text{A2})$$

where p is hourly passenger boarding demand (pass/hr), n is the number of stops; h is service headway (hr/veh). So, the probability of transit stopping at a stop is given as $(1 - e^{(-\lambda)})$ where $\lambda = 2ph/n$. In Equation (A2), the upper limit indicates that transit stops at all stop locations (n) in a high demand case, and the lower limit indicates that for a very low passenger demand condition, the passengers tend to board and alight at distinct stop locations. For this study, a low demand route with an average hourly demand of only 9 pass/hr is selected for analysis; therefore, the lower limit expression is used to estimate $E(s)$.

Appendix B

Using the simplified velocity profile in [Figure B1](#), E_{Prop} can be estimated using known parameters and the trip variables from the real-world data set and consists of three phases: acceleration, coasting, and deceleration as given in Equation (B1) -(B3) adopted from [Gallet et al. \(2018\)](#).

$$E_{Prop}^{acceleration} = l_0(Mgf_r \cos(\theta) + Mgsin(\theta) + 0.5\rho C_d A_f al_0 + \delta Ma) \quad (B1)$$

$$E_{Prop}^{deceleration} = l_0(Mgf_r \cos(\theta) + Mgsin(\theta) - 0.5\rho C_d A_f al_0 + \delta M(-a)) \quad (B2)$$

$$E_{Prop}^{coasting} = l_0(Mgf_r \cos(\theta) + Mgsin(\theta) - 0.5\rho C_d A_f V_R^2) \quad (B3)$$

E_{Prop} between two consecutive stops is estimated based on the following four assumptions:

- (i) the grading is insignificant and can be neglected ($\theta = 0$)
- (ii) the flow velocity of air around the vehicle is equal to the vehicle speed; thus, wind speed is neglected,
- (iii) for a low demand route, the distance between two stoppings is long enough for the coasting speed V_R to be reached.
- (iv) the rate of acceleration denoted by 'a' is equal to the rate of deceleration but with a negative sign.

On applying assumptions on Equation (B1) - (B3), we derive the final expression for E_{Prop} in Equation [\(B4\)](#) given as the sum of energy consumption during acceleration, coasting, and deceleration.

$$E_{Prop} = 2l_0(Mgf_r) + (l - 2l_0)(Mgf_r + 0.5\rho C_d A_f V_R^2) \quad (B4)$$

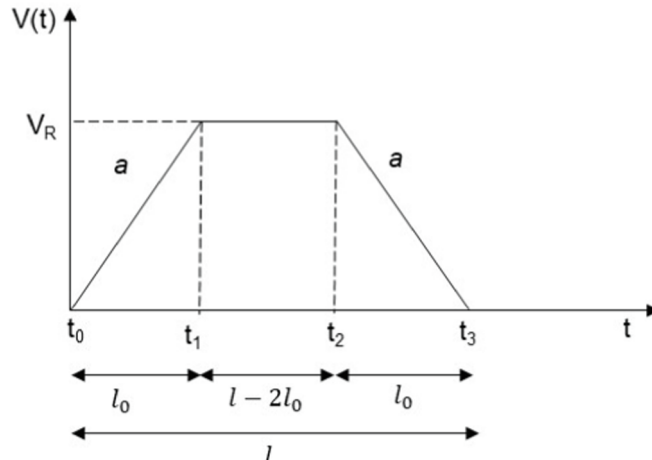


Fig. B1. Simplified speed profile

Appendix C

Table C1

Parameters used in this case study depending on propulsion type, charging scheme, and vehicle type.

Symbol	Unit	ICEV			BEV with opportunity		
		Minivan	Van	Minibus	Minivan	Van	Minibus
C	pass	7	15	25	7	15	25
C_1	\$/veh-hr	13.389 ^[1]	14.049 ^[1]	14.879 ^[1]	13.760 ^[1]	15.122 ^[1]	16.825 ^[1]
C_2	\$/veh-km	0.106 ^[1]	0.229 ^[1]	0.380 ^[1]	0.031 ^[1]	0.066 ^[1]	0.110 ^[1]
C_3	\$/kWh-hr	—	—	—	0.025 ^[1]	0.025 ^[1]	0.025 ^[1]
C_4	\$/charger-hr	0.138 ^[1]	0.138 ^[1]	0.138 ^[1]	8.008 ^[1]	8.008 ^[1]	8.008 ^[1]
$\sum_{x \in X} Z_x \epsilon_x$	\$/veh-km	0.105 ^[1]	0.225 ^[1]	0.375 ^[1]	0	0	0
B_{Chg}	kWh/min	—	—	—	7.5 ^[2]	7.5 ^[2]	7.5 ^[2]
A_f	m ²	2.5 ^[3]	5 ^[3]	6 ^[3]	2.5 ^[3]	5 ^[3]	6 ^[3]
M_{curb}	kg	1500 ^[4]	3000 ^[4]	5000 ^[4]	1500 ^[4]	3000 ^[4]	5000 ^[4]
P_{aux}	kW	—	—	—	0.270 ^[4]	1.600 ^[4]	2.650 ^[4]
P_{others}	kW	—	—	—	0.05 ^[3]	0.05 ^[3]	0.05 ^[3]
$E_{b,nominal}$	kWh	—	—	—	25	25	25

[1] [Barraza and Estrada \(2021\)](#) - Unit costs are estimated in CAD assuming a linear relationship between values and vehicle capacity.

[2] [Estrada et al.\(2022\)](#).

[3] Assumed based on multiple studies.

[4] Average parameter values adopted from [Abdelaty and Mohamed \(2021\)](#) and values for vehicle type estimated using linear relationship.

Table C2

Constant parameters used in the case study.

<i>L</i>	<i>W</i>	<i>V_R</i>	<i>V_a</i>	<i>P</i>	<i>a</i>	<i>t_d</i>	<i>T_L</i>	<i>α, β</i>	<i>L_D</i>	<i>g</i>	<i>m_{pass}</i>	<i>f_r</i>	<i>C_d</i>	<i>ρ</i>	<i>SoC_{min}</i>	<i>C₅</i>	<i>H</i>	<i>T_{preposition}</i>
km 13 ^[1]	km 1 ^[2]	km/hr 35 ^[2]	km/hr 4 ^[2]	pass/hr 9 ^[1]	m/s ² 1 ^[2]	sec 5 ^[2]	min 5 ^[2]	— 0.5 ^[2]	km 0 ^[2]	m/s ² 9.81 ^[3]	kg 75 ^[3]	— 0.008 ^[3]	— 0.7 ^[3]	kg/m ³ 1.18 ^[3]	— 0.2 ^[2]	\$/pass-hr 43.58 ^[2]	hr 12 ^[2]	sec 30

^[1] City of Regina transit ridership data.^[2] Assumed based on research articles and study reports published by government and non-government organizations.^[3] Gallet et al. (2018).

Appendix D

Table D1

List of important parameters.

Notation	Unit	Definition
L	km	Length of the bus route/study area
W	km	Width of the study area
L_D	km	Deadheading distance from terminal stop to the charging station
C_{OC}	\$/hr	operator cost
C_{UC}	\$/hr	user cost
C_{ENV}	\$/hr	environment cost
C_{TC}	\$/hr	total cost
C	pass/veh	vehicle capacity
h	hr/veh	service headway
T_S	hr	slack time to serve route deviation requests
P	pass/hr	average hourly passenger demand along the route
C_1	\$/veh-hr	unit temporal cost
C_2	\$/veh-km	unit distance cost
C_3	\$/kWh-hr	unit temporal battery cost
C_4	\$/charger-hr	unit charging facility cost or refueling station cost
F	veh	fleet size
L_F	veh-km/hr	vehicle kilometers travelled by fleet per unit time
E_b	kWh /veh	battery capacity per vehicle
N_{st}	–	number of charging or refuelling stations
T_C	hr	cycle time
T_O	hr	time required to serve on-route requests
T_{refuel}	hr	time required for refueling in case of ICEV
T_{Chg}	hr	time required for recharging in case of BEV
T_L	hr	Fixed layover time at terminal stations
N_{RD}	–	number of route deviation requests that can be accommodated for a fixed amount of slack time built into the timetable
V_R	km/hr	vehicle riding speed
a	km/hr ²	vehicle acceleration/deceleration rate
t_d	hr	per passenger boarding/alighting time
ϕ	hr	average time required to serve one route deviation request
γ_1	–	proportion for passengers with Type 1 boarding/alighting request
γ_2	–	proportion for passengers with Type 2 boarding/alighting request
γ_3	–	proportion for passengers with Type 3 boarding/alighting request
γ_4	–	proportion for passengers with Type 4 boarding/alighting request
$T_{preposition}$	hr	prepositioning time
E_C	kWh/veh-km	energy consumption factor
P_{aux}	kW	auxiliary power
B_{Chg}	kWh/h	charging speed
S	–	number of trips served before recharging operation
H	hr	service hours per day
E_b	kWh	battery capacity of the vehicle
SoC_{min}	–	minimum state of charge of the batteries
l	km	inter-stop distance
l_0	km	distance covered while accelerating/decelerating the vehicle
M	kg	total mass of vehicle
N_{batt}	–	number of batteries
$E_{b,nominal}$	kWh	nominal capacity of the battery
C_{AT}	\$/hr	access/egress time cost
C_{WT}	\$/hr	waiting time cost
C_{IT}	\$/hr	in-vehicle time cost
V_a	km/hr	passenger walking speed
C_5	\$/pass-hr	passenger value of time
α	–	proportion of planning passengers
β	–	proportion of planning passengers with fixed arrival times

References

- Abdelaty, H., Mohamed, M., 2021. A prediction model for battery electric bus energy consumption in transit. *Energies (basel)* 14, 2824. <https://doi.org/10.3390/en14102824>.
- Alshalafah, B.W., 2009. Planning, design and scheduling of flex-route transit service. University of Toronto, Toronto, CA. Ph.D. Thesis.
- Ansari Esfeh, M., Wirasinghe, S.C., Saidi, S., Kattan, L., 2021. Waiting time and headway modelling for urban transit systems – a critical review and proposed approach. *Transp Rev* 41, 141–163. <https://doi.org/10.1080/01441647.2020.1806942>.

- Badia, H., Jenelius, E., 2021. Design and operation of feeder systems in the era of automated and electric buses. *Transp Res Part A Policy Pract* 152, 146–172. <https://doi.org/10.1016/j.tra.2021.07.015>.
- Barraza, O., Estrada, M., 2021. Battery electric bus network: efficient design and cost Comparison of different powertrains. *Sustainability* 13, 4745. <https://doi.org/10.3390/su13094745>.
- Basma, H., Mansour, C., Haddad, M., Nemer, M., Stabat, P., 2020. Comprehensive energy modeling methodology for battery electric buses. *Energy* 207, 118241. <https://doi.org/10.1016/j.energy.2020.118241>.
- Bektaş, T., Demir, E., Laporte, G., 2016. Green vehicle routing. In: Psarafitis, H.N. (Ed.), *Green Transportation Logistics: the Quest for Win-Win Solutions*. Springer International Publishing, Cham, pp. 243–265. https://doi.org/10.1007/978-3-319-17175-3_7.
- Bösch, P.M., Becker, F., Becker, H., Axhausen, K.W., 2018. Cost-based analysis of autonomous mobility services. *Transp Policy (oxf)* 64, 76–91. <https://doi.org/10.1016/j.tranpol.2017.09.005>.
- Cuta, 2015. *Canadian transit fact book 2015 operating data*. Ontario, Canada, Toronto.
- Daganzo, C., 2005. Logistics systems analysis. Springer Science & Business Media. <https://doi.org/10.1007/3-540-27516-9>.
- Diana, M., Quadrifoglio, L., Pronello, C., 2007. Emissions of demand responsive services as an alternative to conventional transit systems. *Transp Res D Transp Environ* 12, 183–188. <https://doi.org/10.1016/j.trd.2007.01.009>.
- Estrada, M., Salanova, J.M., Medina-Tapia, M., Robusté, F., 2021. Operational cost and user performance analysis of on-demand bus and taxi systems. *Transportation Letters* 13, 229–242. <https://doi.org/10.1080/19427867.2020.1861507>.
- Estrada, M., Mensión, J., Salicrú, M., Badia, H., 2022. Charging operations in battery electric bus systems considering fleet size variability along the service. *Transp Res Part C Emerg Technol* 138, 103609. <https://doi.org/10.1016/j.trc.2022.103609>.
- Fu, L., 2002. Planning and design of flex-route transit services. *Transp Res Rec* 1791, 59–66. <https://doi.org/10.3141/1791-09>.
- Gallet, M., Massier, T., Hamacher, T., 2018. Estimation of the energy demand of electric buses based on real-world data for large-scale public transport networks. *Appl Energy* 230, 344–356. <https://doi.org/10.1016/j.apenergy.2018.08.086>.
- Hjellkrem, O.A., Lervåg, K.Y., Babri, S., Lu, C., Södersten, C.-J., 2021. A battery electric bus energy consumption model for strategic purposes: validation of a proposed model structure with data from bus fleets in China and Norway. *Transp Res D Transp Environ* 94, 102804. <https://doi.org/10.1016/j.trd.2021.102804>.
- Islam, A., Lownes, N., 2019. When to go electric? a parallel bus fleet replacement study. *Transp Res D Transp Environ* 72, 299–311. <https://doi.org/10.1016/j.trd.2019.05.007>.
- Ke, B.-R., Chung, C.-Y., Chen, Y.-C., 2016. Minimizing the costs of constructing an all plug-in electric bus transportation system: a case study in Penghu. *Appl Energy* 177, 649–660. <https://doi.org/10.1016/j.apenergy.2016.05.152>.
- Kikuchi, S., Vuchic, V.R., 1982. Transit vehicle stopping regimes and spacings. *Transp. Sci.* 16, 311–331.
- Kim, M., Levy, J., Schonfeld, P., 2019. Optimal zone sizes and headways for flexible-route bus services. *Transp. Res. B Methodol.* 130, 67–81. <https://doi.org/10.1016/J.TRB.2019.10.006>.
- Koffman, D., 2004. Operational experiences with flexible transit services, TCRP Synthesis 53, TCRP Synthesis 53. Washington, D.C.
- Li, J.-Q., 2016. Battery-electric transit bus developments and operations: a review. *Int J Sustain Transp* 10, 157–169. <https://doi.org/10.1080/15568318.2013.872737>.
- Liu, Z., Song, Z., He, Y., 2019. Economic analysis of on-route fast Charging for battery electric buses: case study in Utah. *Transp Res Rec* 2673, 119–130. <https://doi.org/10.1177/0361198119839971>.
- Ma, T.-Y., Fang, Y., 2022. Survey of charging management and infrastructure planning for electrified demand-responsive transport systems: methodologies and recent developments. *Eur. Transp. Res. Rev.* 14, 36. <https://doi.org/10.1186/s12544-022-00560-3>.
- Mehran, B., Yang, Y., Mishra, S., 2020. Analytical models for comparing operational costs of regular bus and semi-flexible transit services. *Public Transport* 12, 1–23. <https://doi.org/10.1007/s12469-019-00222-z>.
- Militão, A.M., Tirachini, A., 2021. Optimal fleet size for a shared demand-responsive transport system with human-driven vs automated vehicles: a total cost minimization approach. *Transp Res Part A Policy Pract* 151, 52–80. <https://doi.org/10.1016/j.tra.2021.07.004>.
- Mishra, S., Mehran, B., 2023. Optimal Design of Integrated Semi-Flexible Transit Services in low-demand conditions. *IEEE Access* 11, 30591–30608. <https://doi.org/10.1109/ACCESS.2023.3260727>.
- Mishra, S., Mehran, B., Sahu, P.K., 2023. Optimization of headway and bus stop spacing for low demand bus routes. *Transp. Plan. Technol.* 1–26 <https://doi.org/10.1080/03081060.2023.2231429>.
- Mishra, S., Mehran, B., 2023. Effect of stochastic vehicle arrival and passenger demand on semi-flexible transit design. *Public Transport*. <https://doi.org/10.1007/s12469-023-00325-8>.
- Mishra, S., Mehran, B., Sahu, P.K., 2020. Assessment of delivery models for semi-flexible transit operation in low-demand conditions. *Transp Policy (oxf)* 99, 275–287. <https://doi.org/10.1016/j.tranpol.2020.09.004>.
- Mohamed, M., Ferguson, M., Kanaroglou, P., 2018. What hinders adoption of the electric bus in Canadian transit? perspectives of transit providers. *Transp Res D Transp Environ* 64, 134–149. <https://doi.org/10.1016/j.trd.2017.09.019>.
- Schlüter, J., Bossert, A., Rössy, P., Kersting, M., 2021. Impact assessment of autonomous demand responsive transport as a link between urban and rural areas. *Res. Transp. Bus. Manag.* 39, 100613 <https://doi.org/10.1016/j.rtbm.2020.100613>.
- Schroeder, A., Traber, T., 2012. The economics of fast charging infrastructure for electric vehicles. *Energy Policy* 43, 136–144. <https://doi.org/10.1016/j.enpol.2011.12.041>.
- Sung, Y.-W., Chu, J.C., Chang, Y.-J., Yeh, J.-C., Chou, Y.-H., 2022. Optimizing mix of heterogeneous buses and chargers in electric bus scheduling problems. *Simul Model Pract Theory* 119, 102584. <https://doi.org/10.1016/j.simpact.2022.102584>.
- Tirachini, A., Antoniou, C., 2020. The economics of automated public transport: effects on operator cost, travel time, fare and subsidy. *Econ. Transp.* 21, 100151 <https://doi.org/10.1016/j.ecotra.2019.100151>.
- Weiner, R., 2008. Integration of paratransit and fixed-route transit services- TCRP synthesis 76. *Transp. Res. Board*. <https://doi.org/10.17226/13993>.
- Yoon, G., Chow, J.Y.J., Rath, S., 2022. A simulation sandbox to Compare fixed-route, semi-flexible transit, and on-demand Microtransit system designs. *KSCE J. Civ. Eng.* 26, 3043–3062. <https://doi.org/10.1007/s12205-022-0995-3>.